*Journal of Metals, Materials and Minerals, 36(2), e2388, 2026*

# Novel eco-friendly composites: *Crotalaria pallida* (CP) fiber reinforced guar gum/ polyvinyl alcohol blends for enhanced mechanical and thermal properties

Tirupati Rao BANTU[1,2], Renjis T TOM[3] and Delse P. SEBASIAN[4], and Anitha C KUMAR[5,*]

[1] *Department of Chemistry, Acharya Nagarjuna University, Nagarjuna Nagar, Guntur, Andhra pradesh-522510, India*
[2] *Department of Chemistry, Aditya University, Surampalem-533 437, India*
[3] *Department of Chemistry, St. Joseph's College (Autonomous) Devagiri, Affiliated to University of Calicut, kerala, India*
[4] *Department of Botany, St. Joseph's College (Autonomous) Devagiri, Affiliated to University of Calicut, Kerala, India*
[5] *School of Chemical Sciences, Mahatma Gandhi University, Kottayam, Kerala-686560, India*

***Corresponding author e-mail**: anithackumar@mgu.ac.in

**Received date:**
1 May 2025
**Revised date:**
2 July 2025
**Accepted date:**
30 October 2025

**Keywords:**
Sustainable materials;
Biopolymer composites;
*Crotalaria pallida*;
Guar gum;
Polyvinyl alcohol

**Abstract**

Eco-friendly composites exhibit promising applications in wound dressings, tissue engineering, sustainable packaging, and environmental cleanup. This study investigates the development of novel biodegradable composites utilizing guar gum (GG), polyvinyl alcohol (PVA), and *Crotalaria pallida* (CP) fibers, along with wood and nanocellulose, and their characterization. The integration of natural and synthetic polymers with plant fibers enhances mechanical strength, thermal stability, and water resistance. In this study, different loadings of CP material (0.0 g, 0.50 g, 0.75 g, and 1.0 g) and constant amounts of GG and PVA were used to fabricate hybrid films. Fourier Transform Infrared Spectroscopy (FT-IR) analysis revealed significant shifts in –OH and C=O stretching vibrations, indicating strong intermolecular interactions among GG, PVA, and the reinforcements. Scanning Electron Microscopy (SEM) confirmed well dispersed, compact, and cohesive structures, particularly in fiber and nanocellulose based films. Atomic Force Microscopy (AFM) showed an increase in surface roughness for CP fiber composites compared to the pure film, while the wood and nanocellulose composites exhibited relatively smoother surfaces with lower root mean square (RMS) values, suggesting improved matrix uniformity. Tensile strength (TS) analysis demonstrated notable improvements upon fiber addition, with values ranging from 1.7 MPa to 6.7 MPa, indicating that the films are suitable for biodegradable packaging and biomedical applications.

## 1. Introduction

Polymer bio-composites are a sustainable alternative to single use plastics, helping to reduce annual plastic waste by approximately 8 million tons. This reduction helps minimize the accumulation of non-biodegradable waste in landfills and oceans, aligning with the Sustainable Development Goals (SDGs), particularly SDG 12, which promotes sustainable consumption and production patterns [1]. Natural fiber reinforced polymer composites have gained significant attention in recent years due to their sustainability, biodegradability, and eco-friendly nature, serving as a promising alternative to conventional plastics [2-5]. Among these, the incorporation of plant based fibers into polymer matrices has emerged as an effective strategy to enhance the mechanical, thermal, and barrier properties of biodegradable materials [6,7]. GG, a biodegradable polysaccharide, and PVA, a versatile synthetic polymer, combined with the abundant and locally sourced CP materials, provide renewable reinforcement in GG/PVA blends [8-10]. These eco-friendly composites address global environmental concerns, promote sustainable material development, and optimize mechanical and thermal properties, thereby enhancing overall performance [11].

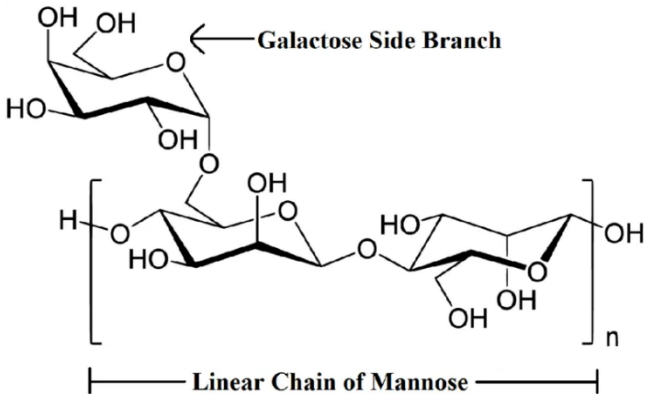


**Figure 1.** Chemical strcture of β-D-mannopyranosyl units linked by (1→4) glycosidic bonds, with α-D-galactopyranosyl units attached through (1→6) linkages (Guar gum).

GG is a high molecular weight galactomannan derived from the seeds of Cyamopsis tetragonoloba. It consists of a linear chain of β-D-mannopyranosyl units linked by (1→4) glycosidic bonds, with α-D-galactopyranosyl units attached through (1→6) linkages [12,13].

Its unique molecular structure imparts excellent water holding capacity, high viscosity, and emulsification properties, making it widely used in food, pharmaceutical, cosmetic, and industrial applications [14]. The thickening, stabilizing, and film forming properties of GG make it a promising candidate for biodegradable films, hydrogel systems, and biopolymer composites [15].

PVA is a hydrophilic polymer known for its superior film forming ability, biocompatibility, and mechanical strength [16,17]. It is produced by the hydrolysis of polyvinyl acetate and is valued for its biodegradability, non-toxicity, and adhesive properties [18]. The enhanced tensile strength, hydrophilic nature, and chemical resistance of PVA make it suitable for use in biodegradable films, coatings, and packaging materials [19]. PVA based composites are increasingly in demand due to their excellent performance, functional versatility, and biodegradability, with potential applications in consumer, biomedical, and agricultural sectors [20].

The combination of GG and PVA provides a unique blend of natural and synthetic polymer properties, making them promising candidates for developing composite materials with tailored performance characteristics [21,22]. Previous research using cellulose, guar gum, and poly(vinyl alcohol) as green solvents has demonstrated the development of environmentally friendly biocomposites exhibiting superior mechanical properties compared to regenerated cellulose [23].

CP, commonly known as smooth rattlebox, is a promising natural fiber source with high cellulose content, low density, and favorable mechanical properties [24,25]. The incorporation of CP fibers is expected to enhance the physicochemical, mechanical, and thermal properties of the resulting composite [9,21]. Moreover, several studies have explored bioplastics as sustainable alternatives to conventional plastics by utilizing plant extracts from guava and chickpea to improve material properties and biodegradability [26].

To the best of our knowledge, no published reports are available on composites comprising GG, PVA, and CP fibers, wood, or nanocellulose. In this work, we have prepared and characterized a novel, eco-friendly composite film composed of GG and PVA reinforced with CP fibers using the solution casting method. The composite films were prepared with constant ratios of GG and PVA while CP materials with different concentrations. We investigated the surface morphology, molecular interactions, and thermal and mechanical properties using SEM, AFM, FT-IR, TS and Thermogravimetric analysis (TGA).

## 2. Experimental

### 2.1 Materials

Guar gum (Galactomannans more than 70%), Polyvinyl alcohol (Molecular weight 60000 g·mol$^{-1}$ to 125000 g·mol$^{-1}$, degree of polymerization 1700 to 1800 and viscosity 9 cps to 21cps), NaOH and Methanol were purchased from HiMedia Laboratories Pvt. Ltd. Borax and Glycerol purchased from Nice Chemicals. 8-Anilino-naphthalene-1-sulfonic acid ammonium salt hydrate (ANS) purchased from sigma-Aldrich and Ethanol (99.9% pure) purchased from Changshu Hongsheng fine chemicals Co. Ltd. Crotalaria Pallida (CP) plant stems were collected from Devagiri, Kerala, India. Milli Q water is used for all the preparations.

### 2.2 Methods

#### 2.2.1 Extraction process of CP fibers

CP, is primarily planted for its fibers, which are utilized in the production of thread, agricultural products, food, and medications. Cold retting with an alkaline hypochlorite solution is used to get the CP fibers. Air dried bast fibers of CP are soaked in 8% NaOH solutions for 48 h, then they are sonicated, washed, and methanol is added to get rid of the lignin. Secondly the acid detergent retting process involves ground alkaline hypochlorite treated plant material, filtered, washed, and dried for removal of hemicellulose. The carboxymethylation process combines acidic detergent treated ground plant fibers with isopropanol and water to modify their surface. This makes soluble and insoluble parts.

#### 2.2.2 Preparation of biodegradable polymer films

Solution casting method was used to prepare bio-composite films. GG (1.0 w/v) solution was prepared by stirring the solution for 24 h continuously with 400 rpm to 500 rpm at 40°C temperature. After GG lumps dissolved completely then the solution is mixed with 1 mL of ANS and 1.0 w/v borax as a cross linker. On other side PVA (4.0 w/v) solution was prepared by continually stirring the mixture for 4 h at 700 rpm to 800 rpm while maintaining a temperature of 70°C to 80°C. Now the resulting solution is mixed with GG and stirred the solution until it is dissolved completely. The mixture is continually agitated for 30 min at 60°C, until a homogeneous solution is achieved. We subjected the solution to sonication for 15 min to remove any air bubbles. After homogenizing the mixture, GG/PVA/CP films were prepared by incorporating CP materials in three different forms i.e. fiber, wood, and nanocellulose at varying loadings of 0.5 g, 0.75 g, and 1.0 g, respectively. The resultant solution is transferred to a 15 cm × 10 cm silicon petri dishes, which is then allowed to dry in a dust free environment for 48 h to produce a self supporting film. The GG/PVA/CP films were extracted and used for subsequent analyses.

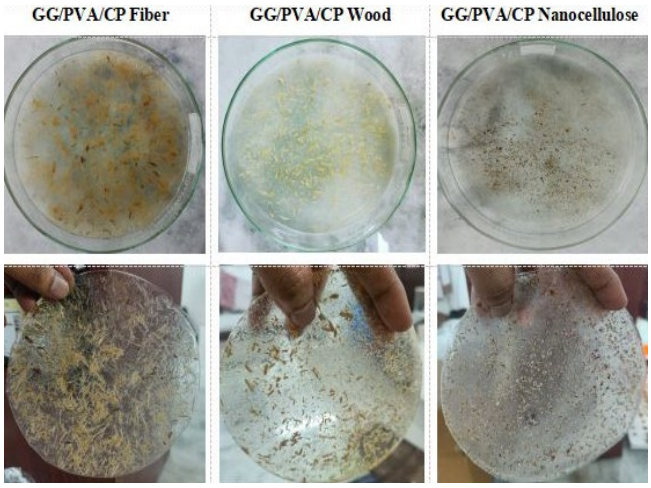


**Figure 2.** Photographic images of GG/PVA/CP fiber, wood and nanocellulose composite films during casting in petri dishes (top row) and after film formation (bottom row).

**Table 1.** The composition of different polymers with natural fibers.

| Sample name | Concentration | | CP materials | Final volume |
|---|---|---|---|---|
| | PVA (4.0 w/v) | GG (1.0 w/v) | [g] | [mL] |
| PG | 4.0 | 1.0 | 0 | 30 |
| PGF-1 | 4.0 | 1.0 | 0.50 | 30 |
| PGF-2 | 4.0 | 1.0 | 0.75 | 30 |
| PGF-3 | 4.0 | 1.0 | 1.00 | 30 |
| PGW-1 | 4.0 | 1.0 | 0.50 | 30 |
| PGW-2 | 4.0 | 1.0 | 0.75 | 30 |
| PGW-3 | 4.0 | 1.0 | 1.00 | 30 |
| PGN-1 | 4.0 | 1.0 | 0.50 | 30 |
| PGN-2 | 4.0 | 1.0 | 0.75 | 30 |
| PGN-3 | 4.0 | 1.0 | 1.00 | 30 |

As shown in the formulation table below, ten different blends were created by adjusting the proportions of PVA, GG, CP fiber, wood and nanocellulose (Table 1). There are four different sets of phrases. For example, sample PG stands for PVA and GG. Polymers with CP fibers are found in PGF-1 to PGF-3; polymers with CP wood components are found in PGW-1 to PGW-3; and polymers with CP nanocellulose are found in samples PGN-1 to PGN-3.

## 2.3 Methods of characterization

### 2.3.1 Film thickness

A thickness meter (thickness measurement gauge digimatic caliper with high accuracy micrometre CD-12"AX, Japan) with a resolution of 0.01 mm and a range of 0 mm to 300 mm was used to measure the thickness of the film. We conducted measurements at four distinct locations.

### 2.3.2 FT-IR analysis

The FT-IR study is used to identify molecular vibrations in GG/PVA and GG/PVA/CP composite films. The FT-IR spectra of the composite films were measured using a PerkinElmer 400 FT-IR spectrometer (IR version 10.6.0) fitted with an ATR attachment. With an average of 16 scans, a small film sample was placed on a "Golden Gate" diamond ATR and examined in the 4000 $cm^{-1}$ to 400 $cm^{-1}$ range using a scanning resolution of 4 $cm^{-1}$ and an interval of 1 $cm^{-1}$.

### 2.3.3 Field emission scanning electron microscopy (FE-SEM)

The surface morphology was examined using field emission scanning electron microscopy (FESEM, TESCAN BRONO s.r.o.Czech). For SEM analysis, a small amount of the film was placed on sticky carbon tape, and the carbon tape was mounted onto an aluminum stud and vacuum coated with gold. SEM images are recorded at 15 kV to 20 kV at different magnifications.

### 2.3.4 AFM analysis

The surface topography of GG/PVA and GG/PVA/CP composite films was measured using a confocal Raman microscope coupled with an AFM (WITecALPHA 300RA). AFM pictures were captured during the tapping step using a silicon tip with a resonance frequency of 75 kHz and a force constant of 2.8 $Nm^{-1}$. AFM images were acquired using a 10 µm × 10 µm scanning size and less than 8 nm radius, processed and analyzed using the WITec Control 4 application.

### 2.3.5 TGA analysis

The thermal degradation of GG/PVA and GG/PVA/CP composite films was examined using the thermogravimetric method. PerkinElmer (TGA 8000) performed the analysis, which has a temperature range of 30°C to 900°C and a heating rate of 10°C·$min^{-1}$. 4 mg to 5 mg of the sample was placed in a platinum crucible and heated at a flow rate of 50 mL·$min^{-1}$ in an inert nitrogen environment in accordance with the instrument specifications. To find the maximal degradation temperature, we used DTG curves.

### 2.3.6 Water solubility (WS)

WS refers to the percentage of the film's dissolved dry matter after immersion in water. The PVA/CS and PVA/CS/CP films were cut to a uniform size (10 mm × 10 mm), dried in an oven at 60°C for 5 h, and then soaked in distilled water at room temperature for 24 h. We collected the leftover sample and used tissue paper to remove the water. Next, we dried the sample at 100°C for 5 h and calculated its solubility. Finally calculated the WS using the following equation.

$$WS\ (\%) = (I_{dw} - F_{dw})/I_{dw} \times 100$$

$I_{dw}$ = Initial dry weigh
$F_{dw}$ = Final dry weight

### 2.3.7 Mechanical properties

The TS and elongation at break (EAB) were measured using a Universal Testing Machine (UTM) (AGS-X series 5 kN, Shimadzu). The tensile speed was set to 30 mm·$min^{-1}$ at ambient temperature. Tensile tests were performed five times for each sample after cutting it into 10 cm × 1.5 cm rectangles.

# 3. Results and discussion

## 3.1 Measuring film thickness

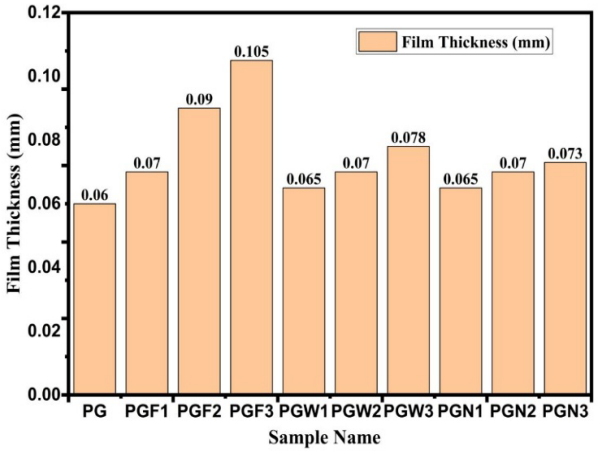


**Figure 3.** Film thickness of various GG/PVA/CP composite films.

During film preparation, molecular arrangement, chemical composition, and solvent interaction influence the thickness of films. Figure 3 shows the appearance and thickness of control and PG active films. Films like PG, PGN, PGW, and PGF appear smooth, homogeneous, and easily removable from petri dishes. The control film (PG), made from PVA and GG, showed the least thickness due to strong hydrogen bonding and the absence of fillers, allowing dense matrix packing. In PGF films, thickness increased significantly with fiber loading because of the bulky, irregular structure of CP fibers that disrupted polymer packing and created voids. PGW films, reinforced with wood, showed moderate thickness; the finer particles dispersed better but contributed less to swelling due to partial interaction and lignin content. PGN films exhibited only slight thickness increases as CP nanocellulose dispersed uniformly and bonded well with the matrix, maintaining compactness with minimal bulk addition [27].

## 3.2 FT-IR results

FT-IR spectroscopy was used to investigate the chemical interactions in GG/PVA/CP composite films. Figure 4(a-c) illustrates the FT-IR spectra of GG/PVA blend films reinforced with various CP fiber (PGF series), wood (PGW series), and nanocellulose (PGN series). Figure 4(a) displays the spectra for the control film (PG) and fiber loaded samples (PGF1, PGF2, PGF3). A broad band at 3289 $cm^{-1}$ to 3268 $cm^{-1}$ corresponds to O–H stretching, indicating the presence of hydroxyl groups from PVA, GG, and CP fibers. The shift and broadening of this peak in PGF samples suggest enhanced hydrogen bonding between the fibers and polymer matrix. The peak around 2903 $cm^{-1}$ to 2915 $cm^{-1}$, attributed to C–H stretching of $–CH_2$ groups, remains stable across all samples, indicating structural integrity of the polymer backbone. A band at 1652 $cm^{-1}$ to 1654 $cm^{-1}$ corresponds to C=O stretching, which becomes more defined in PGF2 and PGF3, suggesting dipole-dipole interactions between carbonyl groups and fiber surfaces [28,29].

**Table 2.** FT-IR Spectral data of GG/PVA/CP fiber, wood and nanocellulose composites (PGF, PGW, PGN).

| Wavenumber [$cm^{-1}$] | Functional group/ vibration | PG (Neat blend) | PGF series (Fiber reinforced) | PGW Series (Wood reinforced) | PGN Series (Nanocellulose-reinforced) | Interpretation |
|---|---|---|---|---|---|---|
| 3309-3256 | O–H and N–H stretching | Broad, centered at 3309 | Broadened and shifted to 3289-3268 | Broadened to 3275 | Broadened to 3256 | Indicates enhanced hydrogen bonding between polymer and natural reinforcements |
| 2934-2915 | C–H stretching (aliphatic $CH_2$) | Medium intensity | Present | Present | Present | Reflects polymer backbone and cellulose structure |
| 1652-1620 | Amide (C=O stretching) / H–O–H bending | Moderate intensity | Slight shift | Slight shift | Slight shift | Change indicates altered hydrogen bond environment due to filler incorporation |
| 1414-1416 | $CH_2$ bending / symmetric $COO^-$ stretching | Weak-moderate | Present | Present | Present | Minor variations suggest structural adjustment |
| 1257-1258 | C–O–C / C–N stretching (glycosidic/ ether linkages) | Weak | Slight shift | Slight shift | Slight shift | Represents polysaccharide bonding (guar gum, cellulose) |
| 1082-1016 | C–O and C–O–C stretching (PVA, guar gum, cellulose) | Strong at 1082 | Increased intensity | Increased | Increased | Confirms presence of polysaccharide rich reinforcements |
| 845-817 | C–H out-of-plane bending (β-glycosidic linkages in cellulose) | Weak | More intense | More intense | Slightly increased | Stronger in fiber and wood composites due to cellulose contribution |

The FT-IR spectra of the GG/PVA/CP wood composites (PGW1, PGW2, PGW3), as shown in Figure 4(b), reveal structural and chemical interactions between the components. A broad peak around 3270 $cm^{-1}$ to 3283 $cm^{-1}$ corresponds to O–H stretching, which becomes more intense in PGW2 and PGW3, indicating enhanced hydrogen bonding due to the addition of CP wood. Peaks at 2915 $cm^{-1}$ to 2909 $cm^{-1}$ (C–H stretching) and 1652 $cm^{-1}$ to 1636 $cm^{-1}$ (C=O stretching) show slight shifts, suggesting interactions among the polymer chains and wood fibers. The C–O stretching band at 1257 $cm^{-1}$ remains stable, confirming the integrity of the polymer backbone. A notable increase in intensity at 1082 $cm^{-1}$ in PGW2 and PGW3 indicates the presence of cellulose and hemicellulose from CP wood. Additionally, peaks around 843 $cm^{-1}$ to 845 $cm^{-1}$ confirm the presence of lignin. These changes confirm the successful incorporation of CP wood into the matrix, leading to improved compatibility and interaction within the composite [30].

The FT-IR spectra of the GG/PVA/CP nanocellulose composites (PGN1, PGN2, PGN3), as shown in Figure 4(c), display characteristic peaks indicating strong interactions between the components. A broad O–H stretching band appears around 3266 $cm^{-1}$ to 3256 $cm^{-1}$, which becomes slightly broader and shifts to lower wavenumbers in PGN3, suggesting enhanced hydrogen bonding due to increased nanocellulose content. The C–H stretching bands between 2934 $cm^{-1}$ and 2921 $cm^{-1}$ indicate the presence of aliphatic groups, with slight shifts reflecting structural rearrangement. The C=O stretching band shifts from 1646 $cm^{-1}$ in PGN1 to 1620 $cm^{-1}$ in PGN3, further confirming hydrogen bond formation [31]. Additionally, strong C–O–C and C–O peaks between 1067 $cm^{-1}$ and 1016 $cm^{-1}$ confirm the successful incorporation of cellulose. These spectral changes support the conclusion that nanocellulose was effectively blended with the GG/PVA matrix, leading to improved interaction and compatibility among the components [32].

The clear spectral differences observed in Figure 4(a-c) confirm the successful incorporation of CP fiber, wood, and nanocellulose into the GG/PVA matrix. Shifts in O–H, C–H, C=O, and C–O–C bands provide evidence of strong hydrogen bonding and chemical compatibility, with each type of filler contributing distinct interactions that affect the composite structure. From the FT-IR data we conclude that hydrogen bonding is the dominant interaction in composite formulations, with cellulose fibers strengthening the GG/PVA matrix.

## 3.3 FE-SEM analysis

A FE-SEM technique was used to analyze the surface morphology and microstructure of GG/PVA and GG/PVA/CP films. Various images show the surface morphology of a sample at a magnification of 1.77x to 600x, and the scale bar indicates a length of 5 µm to 200 µm.

The SEM images of the GG/PVA blends with varying CP fiber loadings are presented in Figure 5(a-d). The pure GG/PVA material's surface should be smooth, indicating a good blend of GG and PVA, with visible interfacial adhesion and no clear phase separation, ensuring a uniform and consistent structure. Figure 5(c-d) shows long, parallel, and interwoven fibers, likely representing a fibrous structure with pores. The fibers have non uniform thickness, with breaks or roughness suggesting structural imperfections. The fibers have varying widths, smooth surfaces, and irregularities, possibly due to defects [33].

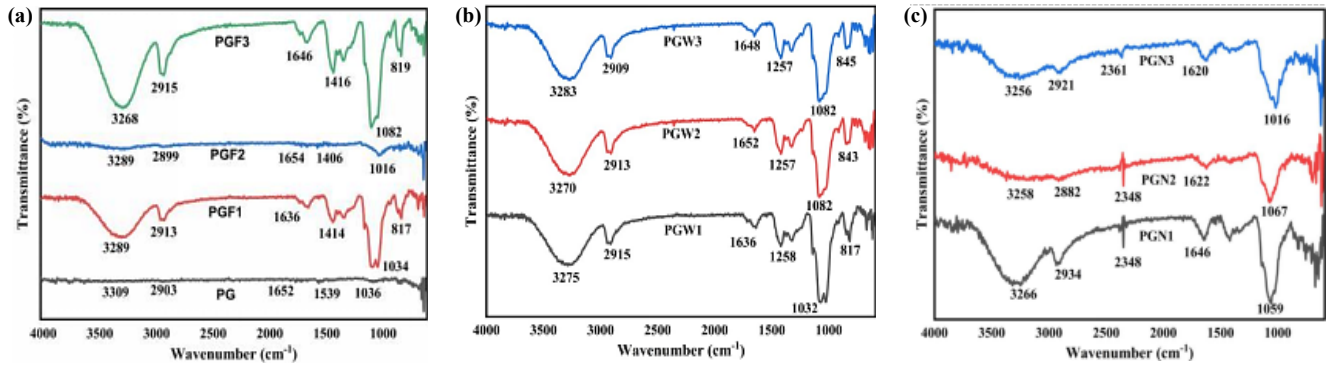


**Figure 4.** FT-IR spectra of (a) GG/PVA/CP fiber, where PG (black), PGF1 (red), PGF2 (blue), and PGF3 (green), (b) GG/PVA/CP wood, where PGW1 (black), PGW2 (red), and PGW3 (blue), and (c) GG/PVA/CP nanocellulose, in which PGN1 (black), PGN2 (red), and PGN3 (blue).

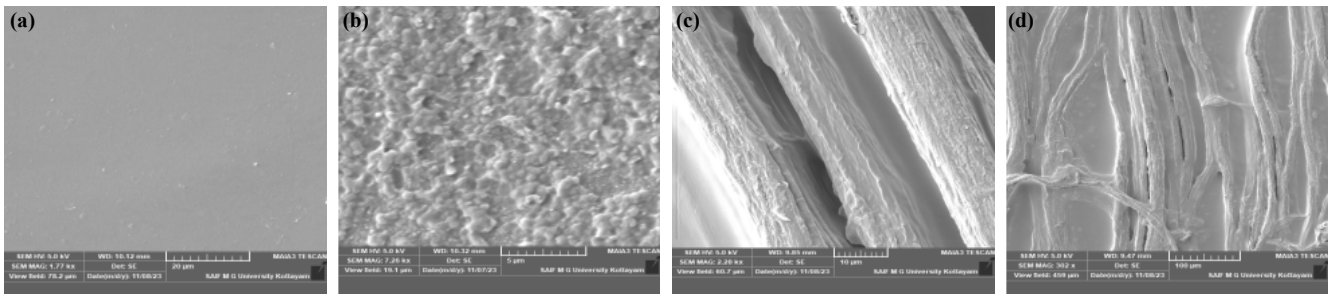


**Figure 5**. SEM micrographs of (a) GG/PVA composite surface at 20 µm scale bar, magnification 1.77 kx, (b) GG/PVA composite at 5 µm scale bar, magnification 7.26 kx, (c) GG/PVA/CP fiber composite at 10 µm scale bar, magnification 2.028 kx, and (d) GG/PVA/CP fiber composite at 100 µm scale bar, magnification 302x.

Figure 6(a-b) indicates that the GG/PVA/CP wood material suggests wood derived cellulose, with visible pores and cracks indicating fiber matrix interactions. The grooves and layered texture suggest incomplete bonding between the polymer and wood fibers. The longitudinal alignment of fibers suggests retained wood structure, potentially improving mechanical properties. Fewer cracks and defects indicate improved dispersion or adhesion [34]. The GG/PVA/CP nanocellulose materials structure is homogeneous, smooth, and compatible, enhancing film flexibility and transparency (Figure 6(c-d)). However, it has a highly porous and fragmented structure, possibly due to nanoparticle agglomeration or weak polymer nanoparticle interactions. This structure is beneficial for applications like biodegradable materials.

The SEM images provide clear insights into the microstructural and interfacial interactions within the composite films. The control film (PG) displays a smooth, compact surface, reflecting strong hydrogen bonding and miscibility between PVA and GG. In contrast, the fiber loaded film (PGF1) shows a rougher morphology, indicating enhanced interfacial adhesion due to fiber matrix entanglement and physical bonding. CP fibers exhibit an irregular, fibrillated surface that promotes mechanical interlocking with the polymer matrix. Similarly, the incorporation of wood particles contributes to interfacial bonding through their lignocellulosic composition specifically via hydrogen bonding between hydroxyl groups of cellulose/hemicellulose and the polymer matrix, as well as physical anchoring due to their rough surface texture [35]. Additionally, nanocellulose enhances binding through its high surface area and abundant hydroxyl groups, leading to dense hydrogen bonding and uniform dispersion within the matrix. Its nanoscale dimensions and high crystallinity further reinforce the composite by improving interfacial load transfer and overall matrix filler compatibility. The increased fiber loading is expected to enhance the tensile strength, flexural strength, and impact resistance of the composites [36].

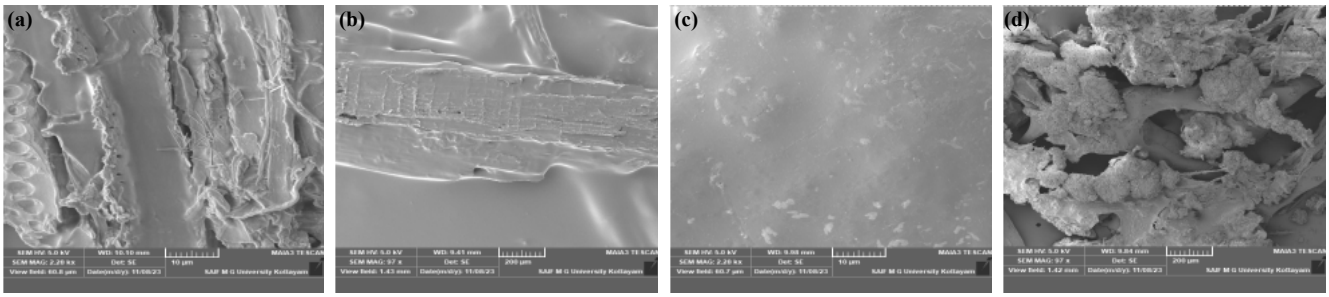


**Figure 6.** SEM micrographs of (a) GG/PVA/CP wood composite at 10 µm scale bar, magnification 2.28 kx, (b) GG/PVA/CP wood composite at 100 µm scale bar, magnification 302x, (c) GG/PVA/CP nanocellulose composite at 10 µm scale bar, magnification 2.28 kx, and (d) GG/PVA/CP nanocellulose composite at 200 µm scale bar, magnification 97x.

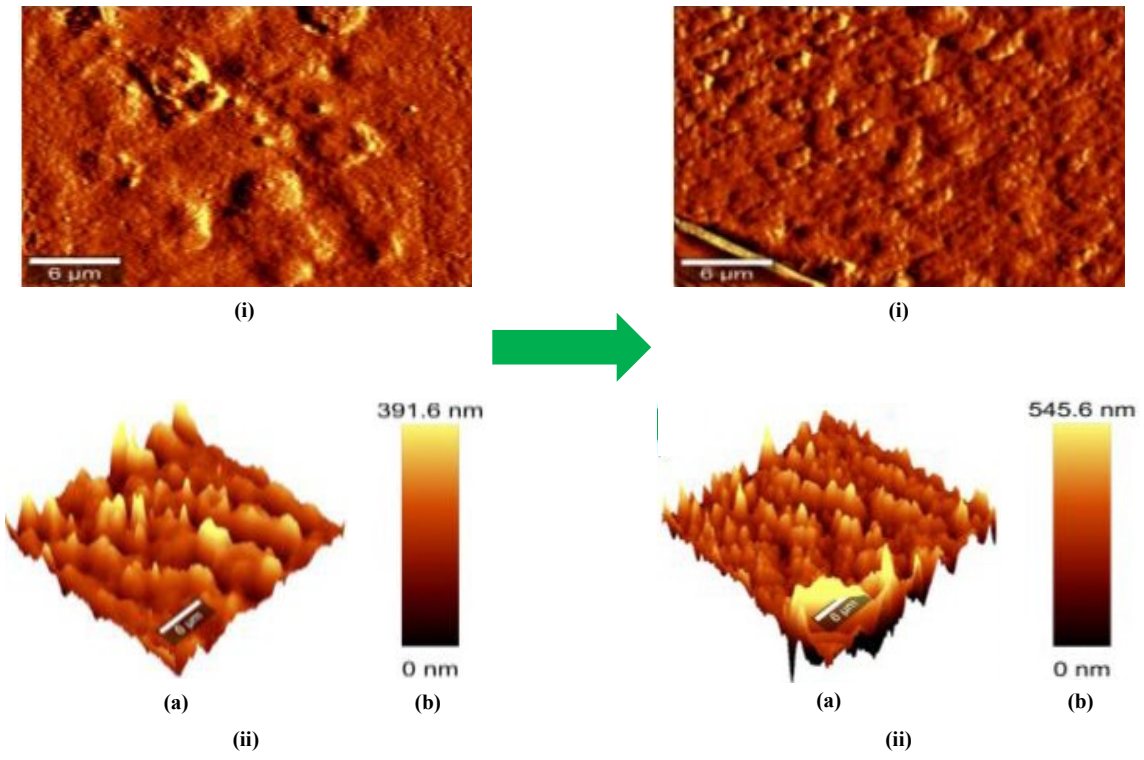


**Figure 7.** AFM images of (i) 2D pure GG/PVA surface at 6 µm scale, (ii) (a) 3D image of pure GG/PVA surface at 6 µm scale, (b) peak height (left) and AFM images of (i) 2D image of GG/PVA/CP fiber film surface at 6 µm scale, (ii) (a) 3D image of GG/PVA/CP fiber film surface at 6 µm scale, (b) peak height (right).

### 3.4 AFM results

The surface topography and roughness of CP fiber reinforced GG/PVA blends were investigated using AFM. The 2D and 3D AFM images (Figure 7, left) depict the surface topography of a GG/PVA composite film, showing a surface height variation from 0 nm to 391.6 nm on a vertical color scale. The surface of the pure GG/PVA matrix appears rough and uneven, with numerous protrusions and depressions, indicating a non-uniform molecular arrangement. In contrast, the surface morphology of the GG/PVA/CP fiber film (Figure 7, right) shows an increase in roughness with a peak height of 545.6 nm compared to the pure film. The image also reveals a more compact surface, suggesting better polymer fiber interaction, which reduces surface fluctuations and enhances the film's structural integrity. AFM analysis of the GG/PVA blending films with CP fibers revealed that surface roughness increased as the CP fiber content grew, indicating improved matrix interaction. The increase in peak height suggests that CP fiber incorporation enhances film homogeneity and compactness, which can lead to improved mechanical properties such as tensile strength and flexibility. This also implies better moisture resistance due to smoother surfaces [37].

Surface roughness was further analyzed using the RMS roughness parameter. The RMS values indicated a smoother surface for the pure GG/PVA film (RMS = 74.978 nm), whereas the RMS value for the 0.5 g CP fiber film was 106.089 nm. These RMS results confirm the improved matrix dispersion in the GG/PVA/CP fiber films [38].

The enhanced surface roughness can provide a larger interfacial area for fiber matrix interactions, leading to improved mechanical strength and stiffness.

### 3.5 TGA analysis

The thermal property of GG/PVA and GG/PVA/CP fiber films was determined by TGA. Figure 8(a) represents the thermal stability based on the 3 stages of weight loss. The initial stage up to 150°C indicates there is a small weight loss (5% to 10%), which corresponds to the evaporation of moisture and volatile components present in the sample [39]. In this stage, both the samples exhibit similar behavior. Secondly, the main stage of decomposition takes place between 200°C and 400°C, resulting in a notable reduction in weight, which indicates that GG and PVA undergo decomposition in this range, which is attributed to the breakdown of polymer chains. The degradation starts slightly earlier for GG/PVA than for GG/PVA/CP fiber, suggesting that the fiber reinforcement slightly enhances thermal stability. The final decomposition stage (400°C to 550°C) shows a slower weight loss phase occurs, attributed to the decomposition of charred residues. The remaining weight percentage approaches zero, indicating nearly complete decomposition. The addition of CP fiber (in the red curve) slightly shifts the degradation temperature to a higher value, suggesting improved thermal stability [40]. GG/PVA/CP fiber has a slightly higher residual weight at the end, possibly due to the char formation from CP fiber.

The derivative weight of GG/PVA and GG/PVA/CP fiber films is shown in Figure 8(b). In all temperature ranges, it is evident that the GG/PVA/CP fiber sample has more thermal stability than GG/PVA, and its decomposition peaks move to slightly higher temperatures. The breakdown of several polymeric components is reflected in the derivative weight peaks, which show multi step degradation. The higher degradation temperatures and larger residual weight indicate that the addition of CP fiber improves thermal stability, according to the TGA results. This implies that CP fiber strengthens the polymer matrix, enhancing its structural integrity and heat resistance.

### 3.6 WS results

Water solubility in a composite film indicates how much of the film degrades or reacts with water. The results show that the pure GG/PVA sample exhibited the highest water solubility, indicating strong hydrophilic behavior. Incorporating CP fiber and wood reduced solubility, enhancing water resistance. Among the composites, wood fiber reinforced films (PGW1-PGW3) demonstrated lower water solubility compared to CP fiber composites, reflecting better moisture resistance. In contrast, CP fiber films (PGF1-PGF3) showed a gradual increase in solubility with higher fiber content, likely due to the hydrophilic nature of the CP fiber itself. Although both fillers influence water uptake, wood fibers contribute more effectively to water resistance than CP fibers [41].

From the data we conclude that higher solubility films like PG are likely to be used in applications where quick degradation is required, while lower solubility films like PGW are better suited for products that need to resist water and maintain their structural integrity over time.

**Table 3.** WS of GG/PVA composite films.

| Sample code | WS [%] |
|---|---|
| PG | 52.28 |
| PGF1 | 30.41 |
| PGF2 | 35.19 |
| PGF3 | 39.91 |
| PGW1 | 25.68 |
| PGW2 | 28.91 |
| PGW3 | 29.33 |

**Table 4.** Mechanical properties of the GG/PVA composite films.

| Sample name | Thickness of the film [mm] | TS [MPa] | EAB [%] |
|---|---|---|---|
| PG | 0.060 | 1.7 | 72 |
| PGW1 | 0.065 | 3.0 | 46 |
| PGF1 | 0.070 | 3.9 | 79 |
| PGW2 | 0.070 | 4.3 | 35 |

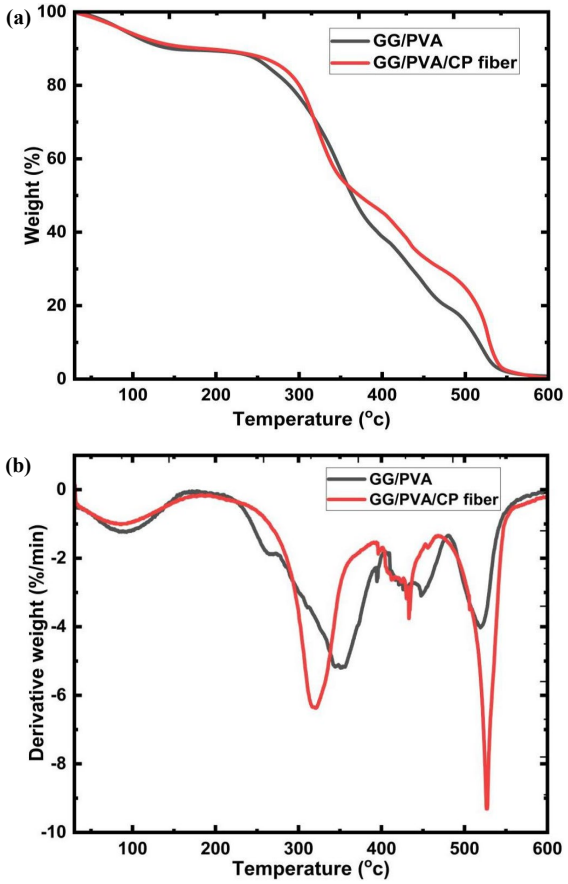


**Figure 8.** TGA thermograms of (a) Weight loss of GG/PVA and GG/PVA/CP fiber films, and (b) Derivative weight of GG/PVA and GG/PVA/CP fiber films.

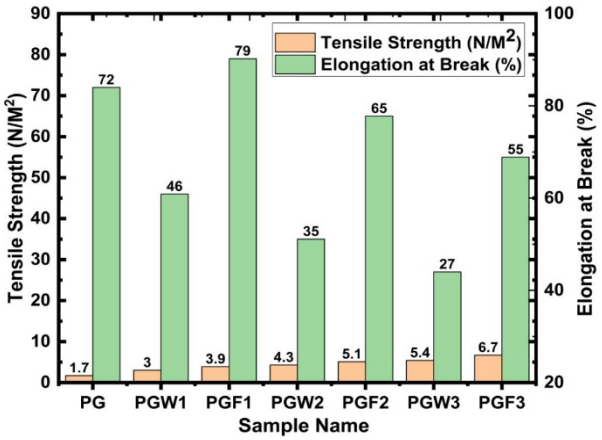


**Figure 9**. Mechanical properties of pure PG, PGF1-PGF3 and PGW1-PGW3 composite films.

### 3.7 Mechanical properties of films

UTM was used to assess the TS and EAB of the GG/PVA blends reinforced with CP fibers and wood materials. GG/PVA composite with CP materials loading (0 g, 0.5 g, 0.75 g, and 1.0 g) was used to measure the TS of the composite films. The mechanical properties of GG/PVA/CP materials summarized in Table 4.

The TS and EAB values of the GG/PVA and the GG/PVA/CP films are shown in Figure 9. The unadulterated GG/PVA film has a tensile strength of 1.7 MPa and an EAB of 72%. When 0.5 g of CP fiber is added, the TS goes up (3.9 MPa) and the elongation increase to 79%, while 0.75 g of CP fiber show increase in tensile strength (5.1 MPa) but decrease in elongation (65%), and 1.0 g of CP fiber loading on film show increases TS (6.7 MPa) but decreases the EAB (55%) [42,43]. The TS of the GG/PVA films was 1.7 MPa, which rise to 3.0 MPa upon the addition of 0.5 g of CP wood. TS was 4.3 MPa by adding 0.75 g of CP wood and 5.4 MPa by adding 1.0 g. As a result, the high surface area of CP wood material leads to an increase in TS when its weight is increased [44]. As a result, hydrogen bonds formed between the GG/PVA matrix and the fiber and wood fillers. The formation of hydrogen bonds enhances the polymer's strength [45]. In this study we found that increasing the fiber composition from 0.5 g to 1.0 g results in an increase in tensile strength but decreases the EaB.

Figure 9 shows the EAB obtained using the CP wood samples PG (72%), PGW1 (46%), PCW2 (37%) and PCW3 (25%). The increase in EAB was due to the molecular relationships between GG/PVA and CP fiber formed by hydrogen bonds. In the GG/PVA/CP fiber samples, the maximum elongation occurs when the fiber portion increases, while in the GG/PVA/CP wood samples, the portion of wood materials reduces the EAB. The TS is influenced by the size of the fiber and wood. When the fibers are modified to the nanometer scale, they show similar mechanical properties to common cellulose fibers because of their larger surface area and active interface. It shows that adding CP fiber as a filler increased the elongation at the break of the GG/ PVA films.

## 4. Conclusion

This study successfully prepared and characterized new eco-friendly composites made from GG and PVA blends reinforced with CP fiber, wood and nanocellulose. The results showed clear improvements in mechanical and thermal properties with more fiber and wood content. The CP fiber film (PGF3) had the highest tensile strength of 6.7 MPa, while the wood film (PGW3) reached 5.4 MPa and was more flexible. Thermal stability also increased, with the decomposition temperature ($T_{50}$) rising from 350°C to 375°C in the CP fiber film. FT-IR analysis revealed significant shifts in –OH and C=O stretching vibrations, indicating strong intermolecular interactions among GG, PVA, and the reinforcements. SEM confirmed well dispersed, compact, and cohesive structures, especially in fiber and nanocellulose reinforced films. These enhancements make the composites promising for sustainable packaging and biomedical use.

## Acknowledgment

Gratitude is extended to all who contributed to the research.

## Conflicts of interest

The authors don't have any conflicts of interest.

## Author contributions

Tirupati Rao Bantu: Writing of original draft, Formal analysis, Conceptualization, Investigation, Methodology, Resource management, Experimental procedures, Visualization, Data curation.

Anitha C Kumar: Writing - Review and editing, supervision, resource management, conceptualization.

T Tom, and Delse P. Sebasian have contributed support in laboratory testing and manuscript preparation.

## References


[1] "Transforming our world: the 2030 Agenda for Sustainable Development | Department of Economic and Social Affairs." https://sdgs.un.org/2030agenda

[2] I. Elfaleh, F.Abbassi, M.Habibi, F. Ahmad, M. Guedri, M. Nasri, and C. Garnier, "A comprehensive review of natural fibers and their composites: An eco-friendly alternative to conventional materials," *Results in Engineering*, vol. 19, p. 101271, 2023.

[3] U. V. Akhil, N. Radhika, B. Saleh, S. A. Krishna, N. Noble, and L. Rajeshkumar, "A comprehensive review on plant-based natural fiber reinforced polymer composites: Fabrication, properties, and applications," *Polymer Composites*, vol. 44, no. 5, pp. 2598–2633, 2023.

[4] V. Prasad, A. A. Vijayakumar, T. Jose, and S. C. George, "A comprehensive review of sustainability in natural-fiber-reinforced polymers," *Sustainability*, vol. 16, no. 3, p. 1223, 2024.

[5] S. Ullah, Z. Akhter, A. Palevicius, and G. Janusas, "Review: Natural fiber-based biocomposites for potential advanced automotive applications," *Journal of Engineered Fibers and Fabrics*, vol. 20, 2025.

[6] M. Mohammed, J. K. Oleiwi, A. M. Mohammed, A. J. Mohamad Jawad, A. F. Osman, and T.Adan, "A review on the advancement of renewable natural fiber hybrid composites: Prospects, challenges, and industrial applications," *Journal of Renewable Materials*, vol. 12, no. 7, pp. 1237–1290, 2024.

[7] S. Nagaraja, P. B. Anand, M. K. K, and M. I. Ammarullah, "Synergistic advances in natural fibre composites: A comprehensive review of the eco-friendly bio-composite development, its characterization and diverse applications," *RSC Advances*, vol. 14, no. 25, pp. 17594–17611, 2024.

[8] D. N. Iqbal, S. Shafiq, S. M. Khan, S. M. Ibrahim, S. A. Abubshait, A. Nazir, and M. Iqbal, "Novel chitosan/guar gum/PVA hydrogel: Preparation, characterization and antimicrobial activity evaluation," *International Journal of Biological Macromolecules*, vol. 164, pp. 499–509, 2020.

[9] T. R. Bantu, and A. C. Kumar, "Polyvinyl alcohol/Chitosan blending films supplemented with *Crotalaria Pallida* fibers: Preparation and Characterization," *RASAYAN Journal of Chemistry*, vol. 18, no. 01, pp. 546–555, 2025.

[10] H. M. Shaikh, A. Anis, A. M. Poulose, N. A. Madhar, and S. M. Al-Zahrani, "Date-palm-derived cellulose nanocrystals as reinforcing agents for poly(vinyl alcohol)/guar-gum-based phase-separated composite films," *Nanomaterials*, vol. 12, no. 7, p. 1104, 2022.

[11] Y. A. Ouma, S. S. Nayak, S. Mishra, and H. Panigrahi, "Bionanocomposites based on polyvinyl alcohol and fuller earth nanoclay: Preparation, properties and its application in food packaging," *Journal of Polymer Materials*, vol. 41, no. 4, pp. 281–297, 2024.

[12] A. P. Gupta, and G. Arora, "Preperation and characterization of cross-linked guar-gum poly(vinylalcohol) green films," *Pelagia Research Library*, vol. 3, no.5, pp.1191-1197, 2012.

[13] D. Mudgil, S. Barak, and B. S. Khatkar, "Guar gum: processing, properties and food applications—A Review," *Journal of Food Science and Technology*, vol. 51, no. 3, pp. 409–418, 2011.

[14] X. Huang, J. Song, F. Xu, D. Yun, C. Li, and J. Liu, "Characterization and application of guar gum/polyvinyl alcohol-based food packaging films containing betacyanins from pokeweed (Phytolacca acinosa Roxb.) berries and silver nanoparticles," *Molecules*, vol. 28, no. 17, p. 6243, 2023.

[15] D. Jussen, S. Sharma, J. K. Carson, and K. L. Pickering, "Preparation and tensile properties of guar gum hydrogel films," *Polymers and Polymer Composites*, vol. 28, no. 3, pp. 180–186, 2019.

[16] M. Yang, Z. Wang, M. Li, Z. Yin, and H. A. Butt, "The synthesis, mechanisms, and additives for bio-compatible polyvinyl alcohol hydrogels: A review on current advances, trends, and future outlook," *Journal of Vinyl and Additive Technology*, vol. 29, no. 6, pp. 939–959, 2022.

[17] B. Tan, Y. Ching, S. Poh, L. Abdullah, and S. Gan, "A review of natural fiber reinforced poly(vinyl alcohol) based composites: Application and opportunity," *Polymers*, vol. 7, no. 11, pp. 2205–2222, 2015.

[18] N. Abinaya, P. Sivaranjana, N. Rajini, and K. Krishnan, "Performance analysis of biodegradable composite using polyvinyl alcohol and pomegranate peel powder for sustainable dry packaging applications," *Discover Materials*, vol. 4, no. 1, 2024.

[19] F. Fitriani, S. Aprilia, M. Mahardika, N. Masruchin, and W. Rinaldi, "Development of hybrid biodegradable polymer based on polyvinyl alcohol and whey protein isolate reinforced with cellulose nanocrystal from pineapple crown Leaf," *Case Studies in Chemical and Environmental Engineering*, vol. 11, p. 101061, 2024.

[20] C. Cao, L. Zhao, and G. Li, "Using polyvinyl alcohol as polymeric adhesive to enhance the water stability of soil and its performance," *arXiv.org*, 2024.

[21] M. Z. Hasan, Y. Arafat, M. M. Bashar, M. N. N. Niloy, M. I. Khandaker, and A. M. S. Chowdhury, "Poly-(vinyl alcohol) composite films reinforced with carboxylated functional microcrystalline cellulose from jute fiber," *Composites and Advanced Materials*, vol. 31, 2022.

[22] M. A. Moghadam, R. Mohammadi, E. Sadeghi, M. A. Mohammadifar, M. Nejatian, M. Fallah, and M. Rouhi, "Preparation and characterization of poly(vinyl alcohol)/gum tragacanth/cellulose nanocomposite film," *Journal of Applied Polymer Science*, vol. 138, no. 28, 2021.

[23] C. M. Patil, A. U. Borse, and J. S. Meshram, "Ionic liquid: Green solvent for the synthesis of cellulose/guar gum/PVA biocomposite," *Green Materials*, vol. 6, no. 1, pp. 23–29, 2018.

[24] Md. Z. Islam, Md. T. Hossain, F. Hossen, S. K. Mukharjee, N. Sultana, and S. C. Paul, "Evaluation of antioxidant and antibacterial activities of *crotalaria pallida* stem extract," *Clinical Phytoscience*, vol. 4, no. 1, 2018.

[25] S. Ukil, S. Laskar, and R. N. Roy, 'Physicochemical characterization and antibacterial activity of the leaf oil of *crotalaria pallida* aiton," *Journal of Meningitis*, vol. 1, no. 3, pp. 1–2, 2016.

[26] S. Elsaeed, E. Zaki, A. Diab, M.-A. Tarek, and W. a. E. Omar, "New polyvinyl alcohol/gellan gum-based bioplastics with guava and chickpea extracts for food packaging," *Scientific Reports*, vol. 13, no. 1, 2023.

[27] V. G. Bhat, S. S. Narasagoudr, S. P. Masti, R. B. Chougale, and Y. Shanbhag, "Hydroxy citric acid cross-linked chitosan/guar gum/poly(vinyl alcohol) active films for food packaging applications," *International Journal of Biological Macromolecules*, vol. 177, pp. 166–175, 2021.

[28] A. F. Lubambo, N. Mattoso, L. Ono, G. G. da Luz, B. Gavinho, A. A. Martin, M. R.Sierakowski, and C. K. Saul, "In situ synthesis of AZO-NP in guar gum/PVOH composite fiber MATs for potential bactericidal release," *Polymers*, vol. 14, no. 22, p. 4983, 2022.

[29] T. Das, S. Yeasmin, S. Khatua, K. Acharya, and A. Bandyopadhyay, "Influence of a blend of guar gum and poly(vinyl alcohol) on long term stability, and antibacterial and antioxidant efficacies of silver nanoparticles," *RSC Advances*, vol. 5, no. 67, pp. 54059–54069, 2015.

[30] K. S. Soppimath, A. R. Kulkarni, and T. M. Aminabhavi, "Controlled release of antihypertensive drug from the inter-penetrating network poly(vinyl alcohol)–guar gum hydrogel microspheres," *Journal of Biomaterials Science Polymer Edition*, vol. 11, no. 1, pp. 27–43, 2000.

[31] R. Vârban, I. Crisan, D. Vârban, A. Ona, L. Olar, A. Stoie and Răzvan Stefan, "Comparative FT-IR prospecting for cellulose in stems of some fiber plants: flax, velvet leaf, hemp and jute," *Applied Sciences*, vol. 11, no. 18, p. 8570, 2021.

[32] M. U. A. Khan, I. Iqbal, M. N. M. Ansari, S. I. A. Razak, M. A. Raza, A. Sajjad , F. Jabeen, M. R. Mohamad, and N. Jusoh, "Development of antibacterial, degradable and ph-responsive chitosan/guar gum/polyvinyl alcohol blended hydrogels for wound dressing," *Molecules*, vol. 26, no. 19, p. 5937, 2021.

[33] Y. Yue, X. Cheng, H. Liu, M. Zang , B. Zhao, X. Zhao and L. Wang, "Gellan gum and polyvinyl alcohol based triple-layer films enriched with alhagi sparsifolia flower extract: preparation, characterization, and application of dried shrimp preservation," *Foods*, vol. 12, no. 21, p. 3979, 2023.

[34] D. N. Iqbal, S. Ehtisham-ul-Haque, S. Ahmad, K. Arif , E. A. Hussain, M. Iqbal , S. Z. Alshawwa, M. Abbas, N. Amjed, and A. Nazir, "Enhanced antibacterial activity of chitosan, guar gum and polyvinyl alcohol blend matrix loaded with amoxicillin and doxycycline hyclate drugs," *Arabian Journal of Chemistry*, vol. 14, no. 6, p. 103156, 2021.

[35] V. N. Vanjeri, V. D. Hiremani, N. Goudar, O. J. D'souza, J. P. Pinto, A. R. Patil, S. S. Narasagoudr, S. P. Masti, and R. B. Chougale, "Assessment of thermal, crystalline and morphological properties of ellagic acid incorporated PVA, chitosan, PVA/chitosan and PVA/chitosan/gaur gum polymeric films," *International Journal of Polymer Analysis and Characterization*, vol. 28, no. 7, pp. 647–661, 2023.

[36] D. N. Iqbal, M. Tariq, S. M. Khan, N. Gull, S. S. Iqbal, A. Aziz, A. Nazir, and M. Iqbal, "Synthesis and characterization of chitosan and guar gum based ternary blends with polyvinyl alcohol," *International Journal of Biological Macromolecules*, vol. 143, pp. 546–554, 2019.

[37] D. Kasai, R. Chougale, S. Masti, R. Chalannavar, R. B. Malabadi, and R. Gani, "Influence of Syzygium cumini leaves extract on morphological, thermal, mechanical, and antimicrobial properties of PVA and PVA/chitosan blend films," *Journal of Applied Polymer Science*, vol. 135, no. 17, 2018.

[38] S. Nokhasteh, A. M. Molavi, M. Khorsand-Ghayeni, and A. Sadeghi-Avalshahr, "Preparation of PVA/Chitosan samples by electrospinning and film casting methods and evaluating the effect of surface morphology on their antibacterial behavior," *Materials Research Express*, vol. 7, no. 1, p. 015401, 2019.

[39] H. a. S. Alhaithloul, I. M. Alsudays, E. G. Zaki, S. M. Elsaeed, A. E. Mubark, L. Salib, G. Safwat, G. Niedbała, A. Diab , M. A. Abdein, A. Alharthi , S. A. Zakai, and A. Elkelish, "Retrieval of $Cu^{2+}$ and $Cd^{2+}$ ions from aqueous solutions using sustainable guar gum/PVA/montmorillonite nanocomposite films: Effect of temperature and adsorption isotherms," *Frontiers in Chemistry*, vol. 12, 2024.

[40] T. S. Anirudhan, S. S. Nair, and C. Sekhar V., "Deposition of gold-cellulose hybrid nanofiller on a polyelectrolyte membrane constructed using guar gum and poly(vinyl alcohol) for trans-dermal drug delivery," *Journal of Membrane Science*, vol. 539, pp. 344–357, 2017.

[41] S. Bhowmik, D. Agyei, and A. Ali, "Biodegradable chitosan hydrogel film incorporated with polyvinyl alcohol, chitooligo-saccharides, and gallic acid for potential application in food packaging," *Cellulose*, vol. 31, no. 13, pp. 8087–8103, 2024.

[42] R. M. A. Syed, N. Nagabhooshanam, B. M. Raj G, R. Verma, D. S. Kumar, B. T. Rao, and D. Sravani, "Effect of vinyl silane–treated plant root waste biomass cellulose on pineapple fiber-vinyl ester composites: A characterization study," *Biomass Conversion and Biorefinery*, vol. 15, no. 7, pp. 10933–10945, 2024.

[43] M. Balasubramanian, N. Nagabhooshanam, G. B. Mohan Raj, R. Verma, D. S. Kumar, B. T. Rao, and D. Sravani, "Effect of vinyl silane-treated Amaranthus spinosus plant root cellulose on load-bearing and time-dependent properties of pineapple fiber–vinyl ester composite," *Polymer Bulletin*, vol. 82, no. 7, pp. 2169–2190, 2024.

[44] L. B. Abhang, T. Subramanian, N. Nagabhooshanam, K. Sharma, P. K. V. Rao, K. M. Devi, and A. L. Lavanya, "Biosynthesize of ZnO nanoparticle from orange fruit peel biomass and its PVA-based composite packaging material: a greener material for suitable packaging," *Biomass Conversion and Biorefinery*, vol. 15, no. 9, pp. 14037–14046, 2024.

[45] H. Farrokhi, M. Koosha, N. Nasirizadeh, M. Salari, M. Abdouss, T. Li, and Y. Gong, "The effect of Nanoclay type on the mechanical properties and antibacterial activity of Chitosan/PVA nanocomposite films," *Journal of Composites Science*, vol. 8, no. 7, p. 255, 2024.